We are IntechOpen,
the world's leading publisher of
Open Access books
Built by scientists, for scientists

6,900
Open access books available

186,000
International authors and editors

200M
Downloads

154
Countries delivered to

Our authors are among the

TOP 1%
most cited scientists

12.2%
Contributors from top 500 universities

CLARIVATE ANALYTICS
BOOK CITATION INDEX
INDEXED

WEB OF SCIENCE™

Selection of our books indexed in the Book Citation Index
in Web of Science™ Core Collection (BKCI)

Interested in publishing with us?
Contact book.department@intechopen.com

Numbers displayed above are based on latest data collected.
For more information visit www.intechopen.com

High-Order Harmonic Generation from Low-Density Plasma

Tsuneyuki Ozaki[1], Rashid Ganeev[1], Masayuki Suzuki[2] and Hiroto Kuroda[2]
[1]Institut national de la recherche scientifique
[2]Institute for Solid-State Physics, University of Tokyo
[1]Canada
[2]Japan

1. Introduction

High-order harmonic generation (HHG) of ultra-short laser pulses is an effective method to generate extreme ultraviolet (XUV) radiation and attosecond light pulses. Currently, various techniques are used for HHG, such as the interaction of intense laser with gases (Kazamias et al., 2003), with low-density laser-produced plasmas (Ganeev, 2007), and by reflecting relativistic intensity laser pulses from solid surfaces (Norreys et al., 1996). Such harmonics are promising sources of coherent soft x-ray radiation with various applications, such as XUV nonlinear optics and spectroscopic studies. In particular, the major advantages of HHG are very good spatial quality and femtosecond to attosecond temporal resolution. Single attosecond XUV pulses (with pulse durations of several hundred attoseconds) from HHG has been generated, by irradiating neon gas atoms with intense, few-cycle laser pulse (Drescher et al., 2001), and the current record for the shortest pulse ever generated is 80 attoseconds (Goulielmakis et al., 2008). Furthermore the maximum cut-off energy of harmonics has been extended up to 1.3 keV (corresponding to a wavelength of 0.95 nm) (Seres et al., 2005). This ultra-short nature of harmonics has lead to several applications of pivotal importance, such as controlling the motion of bound electrons in molecular dissociation (Kling et al., 2006), mapping of attosecond electron wave packet motion (Niikura et al., 2005), and nonlinear phenomena in the XUV region (Nabekawa et al., 2005).

To extend the harmonic cut-off to shorter wavelengths, one needs to use nonlinear medium with higher ionization potential. This is because generally speaking, the harmonic cut-off energy $E_{cut-off}$ is determined by the cut-off rule $E_{cut-off} = I_p + 3.17\,U_p$, where I_p is the ionization potential and U_p the ponderomotive energy (Corkum, 1993). Thus, we should observe increased cut-off energy with increased laser intensity. However, the highest photon energies demonstrated to date by HHG have generally been limited not by the cut-off rule, but by effects that come into play as the gas is ionized by the laser. For example, if the gas medium is ionized before the peak of the laser pulse arrives, the neutral atom can only interact with a lower "saturation intensity", which is the intensity where 98% of the gas is singly ionized. The saturation intensity can be increased using shorter-duration laser pulses or using atoms with a large ionization potential, thus allowing the atoms to survive higher laser intensity before ionizing. For example, instead of rare-gas atoms, rare-gas like ions in

laser-produced plasmas of alkali metal has been used in the past for HHG (Akiyama et al., 1992; Kubodera et al., 1993; Wahlstrom et al., 1995). The basic idea was to capitalize on the high ionization potential of alkali metal, which is higher than those of any other gas atom. The cut-off energies of the HHG using KrF excimer lasers (248 nm wavelength) were 64.92 eV and 105 eV, for potassium (Akiyama et al., 1992) and lead ions (Kubodera et al., 1993) produced in laser-plasmas. On the other hand, experiments using Ti:sapphire lasers as the pump have only demonstrated cut-off up to the 27th harmonic (29.4 nm wavelength) using sodium and potassium ions (Wahlstrom et al., 1995). In all of the above experiments with rare-gas-like ions, the plateau was never observed. Recently, we have demonstrated the 63rd harmonic (12.63 nm wavelength, 98 eV photon energy) using laser ablation boron ions irradiated by 150 fs Ti:sapphire laser pulse (Ganeev et al., 2005d). Experimental evidence show that these harmonics result from the interaction of femtosecond laser pulse with singly charged ions and neutral atoms. In this experiment, the plateau has been observed.

Another important goal of HHG research is to increase its conversion efficiency. In the past, such conversion efficiency enhancement has been pursued by controlling the phase matching condition in gas filled capillary (Rundquist, 1998) or gas cell (Tamaki et al., 1999). Using xenon gas-filled hollow-core fiber, strong 15th harmonic at a wavelength of 53.3 nm was obtained with a conversion efficiency of 4×10^{-5} (Constant et al., 1999). Conversion efficiency of 3×10^{-5} was obtained for the 23rd harmonic at a wavelength of 35 nm, by using argon gas cell (Kazamias et al., 2003). The strongest output energy of harmonics were 7 µJ for the 11th harmonic at a wavelength of 72.7 nm, 4.7 µJ for 13th harmonic at a wavelength of 62.3 nm, and 1 µJ for 15th harmonic at a wavelength of 54 nm using xenon gas cell (Takahashi et al., 2002). More recent results have reported an enhancement of high-order harmonic conversion efficiency when a two-color (fundamental and second harmonic field) orthogonally polarized driving field is used (Kim et al., 2005). In this scheme, the conversion efficiency of the 38th harmonic (21.6 nm) was 5×10^{-5}, using helium gas jet. An alternative approach is to use resonance enhancement in HHG, which has been proposed by theoretical calculations (Gaarde & Schafer, 2001; Faria et al., 2002; Taieb et al., 2003b). Experimentally, resonance enhancement of the 13th and the 15th harmonics using argon gas medium has been observed (Toma et al., 1999). However the enhancement in these works were a factor of two to three, and the harmonic spectrum consisted of multiple harmonics.

In this chapter, we will review recent developments in the generation of intense high-order harmonics using lowly ionized plasma as the nonlinear medium. While early experiments have shown high-order harmonic generation using similar technique (Akiyama et al., 1992; Kubodera et al., 1993; Wahlstrom et al., 1995), the harmonic spectra lacked a plateau, and consequently the cut-off was limited. In contrast, recent results have shown clear plateau (Ganeev et al., 2005d) with a cut-off as high as the 101st order (Ganeev et al., 2007). A unique intensity enhancement of a single high-order harmonic that dominates the spectrum has been observed in the XUV region (Ganeev et al., 2006). Such enhancement of a single harmonic is an advantage for several important applications of coherent XUV radiation. One example is photoelectron spectroscopy for understanding excited-state electron dynamics, in which there is a need to select one harmonic while eliminating neighboring harmonics. This single enhancement technique will allow the generation of a quasi-monochromatic coherent x-ray source, without complexities of using monochromators, multilayer mirrors and filters. Another characteristic of this plasma harmonic method is that one could use any target that

could be fabricated into solids. Profiting from this feature, there has been several works on pioneering high-order harmonic generation from nanostructured material, such as metallic nanoparticles and fullerenes. This chapter is organized as follows. In Section 2, I will review the basic experimental setup for plasma harmonic generation. In Section 3, I will review the various cut-off of plasma harmonics and their relation to the ionization potential of the target material. In Section 4, intensity enhancement of a single harmonic order is discussed, and in Section 5, on high-order harmonics from nanostructured material.

2. Experimental setup

A schematic diagram of the typical experimental setup is shown in Fig. 1. The pump laser is usually a high-intensity femtosecond laser system, such as the Ti:sapphire laser. A pre-pulse is split from the amplified laser beam using a beam splitter before the pulse compressor. The typical pre-pulse energy is 5 - 17 mJ with pulse duration of a few hundred ps. The main femtosecond pump pulse typically has energy of 5 - 17 mJ. A cylindrical or spherical lens focuses the pre-pulse onto a solid target placed within a vacuum chamber, which generates a laser ablation plume that contains low-charged ions. The size of the focus on the target surface is typically 1 mm, and the intensity of the pre-pulse was varied between $10^{10} - 10^{11}$ Wcm^{-2}. The main pulse is focused onto the ablation plasma by a spherical lens, with a delay between 20 to 100 ns after the pre-pulse irradiation. The typical intensity of the main pulse at the plasma plume is $10^{14} - 10^{15}$ Wcm^{-2}. The spectrum of the generated high-order harmonics was measured by grazing incidence spectrometer with a gold-coated Hitachi 1200 grooves/mm flat-field grating (such as the Hitachi 001-437). A gold-coated grazing-incidence cylindrical mirror was used to image the target harmonics at the ablation plume onto detector plane. The XUV spectrum is detected using a two-dimensional x-ray detector
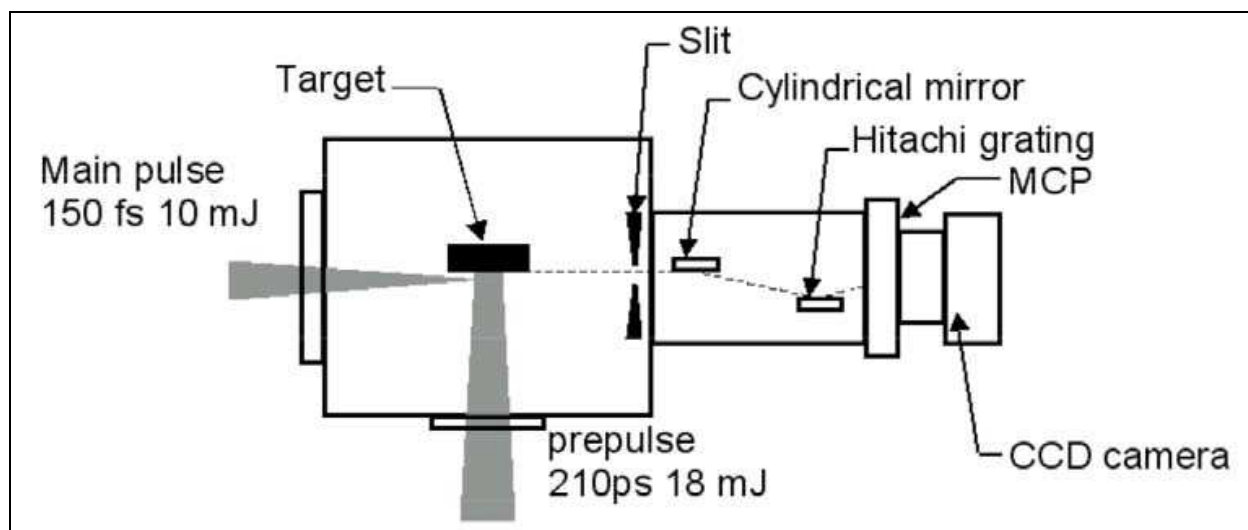

Fig. 1. Schematic of experimental setup for HHG measurement from the laser ablation plume pumped by femtosecond laser pulse. First the prepulse was focused on the target surface. Then the main pulse was focused into the preplasma that was produced by the prepulse. Delay between prepulse and main pulse is 100 ns. The generated high-order harmonics were measured by grazing incidence spectrometer and detected by microchannel plate with CCD camera.

(such as a micro-channel plate with a phosphor screen read-out), and the spectrum is recorded using a CCD camera. To obtain the energy of the harmonics generated, the absolute calibration of the spectrometer system is performed using the following method (Ganeev et al., 2005a)[27]. First, the intensity of the 3rd harmonic generated from a nonlinear crystal is measured, and its readout intensity is compared with that of the 3rd harmonic generated from the laser ablation plasma by using a commercial spectrograph. The intensity of the 3rd harmonic was measured with a power meter. Then, one compares the intensity of the 3rd harmonic with that of the 9th harmonic from the laser ablation plumes using the commercial spectrograph. Finally, one compares the intensity of the 9th harmonic with that of the high-order harmonics in the XUV region using the flat-field spectrometer.

3. Cut-off of plasma harmonics

Figure 2 and 3 shows the typical HHG spectra from silver and vanadium laser ablation plumes. There are two characteristics of these spectra that show them to be harmonics. First, only odd-order harmonics are observed, and second, these harmonics disappear by simply rotating the polarization of the femtosecond laser pulse from linear to circular. The spectrum from vanadium ablation (Fig. 3) shows high-order harmonics up to the 71st order (11.20 nm wavelength). The conversion efficiency of the 71st harmonic was measured to be 1.6×10^{-7}. Using laser plasma of silver (Fig. 2), the cut-off is at the 59th harmonic (13.47 nm) with a conversion efficiency of 6×10^{-6}. Typical plateau and cut-off were observed in both spectra. The appearance of the plateau in the spectrum indicates that these harmonics are generated in the non-perturbative regime. Therefore the cut-off energy of the harmonics from the laser ablation plume could be explained by the three-step model (Corkum, 1993). In the three-step model, the cut-off energy rule is given by $E_{cut-off} = I_p + 3.17 U_p$, [eV]. Here, I_p is the ionization potential of the nonlinear medium, and U_p is the ponderomotive potential, where $U_p = e^2 E^2 / 4 m \omega^2 = 9.33 \times 10^{-14} I \lambda^2$, where e and m are electron charge and mass, and E, ω, I, λ, are the laser field amplitude, laser frequency, laser intensity (in units of Wcm^{-2}) and laser wavelength (in units of μm), respectively. In previous works, a plot of the harmonic cut-off energy as a function of the ionization potential showed that the cut-off depended strongly on the second ionization potential of the ablation atom (Ganeev et al., 2005b). For example, the harmonic cut-off energy for boron was 98 eV (12.6 nm wavelength), which has a second ionization potential of 24.12 eV. For silver, which has a second ionization potential of 21.04 eV, the cut-off was at 95 eV (13.03 nm wavelength), showing high correlation between the two. However, our experimental results with vanadium seem to deviate from this rule. The second ionization potential of vanadium is 14.65 eV, but the cut-off is at the 71st harmonic (11.20 nm wavelength), with photon energy of 110 eV. That is, the second ionization potential of vanadium is lower than that of silver, but the cut-off energy of vanadium is higher than that of silver. The estimated maximum cut-off energy of vanadium was 85.6 eV by using the cut-off rule equation and assuming that the U_p is the same as that of silver. However, experiments show that the cut-off energy is higher than this estimated value. We attribute the observation of the 71st harmonic to the contribution from doubly charged ions. The third ionization potential of vanadium is 29.31 eV, which is higher than the second ionization potential value of boron. Therefore the observation of cut-off energy by using vanadium is higher than that of boron.
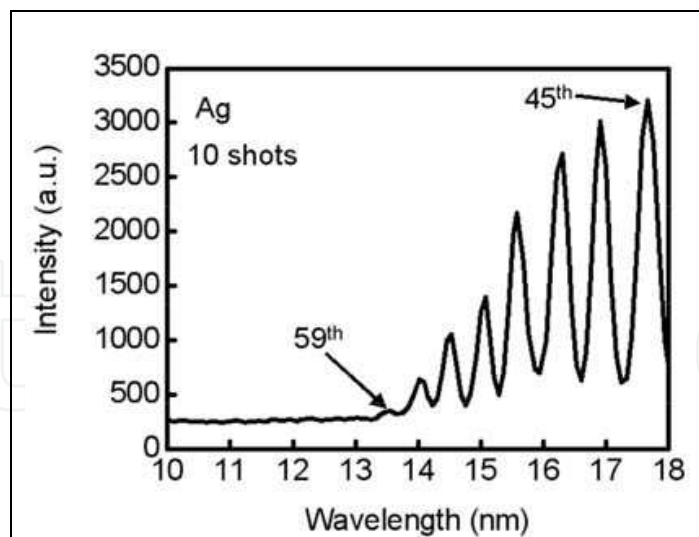
Fig. 2. HHG from the laser ablation silver plume, with a cut-off at the 59th harmonic (13.47 nm wavelength).
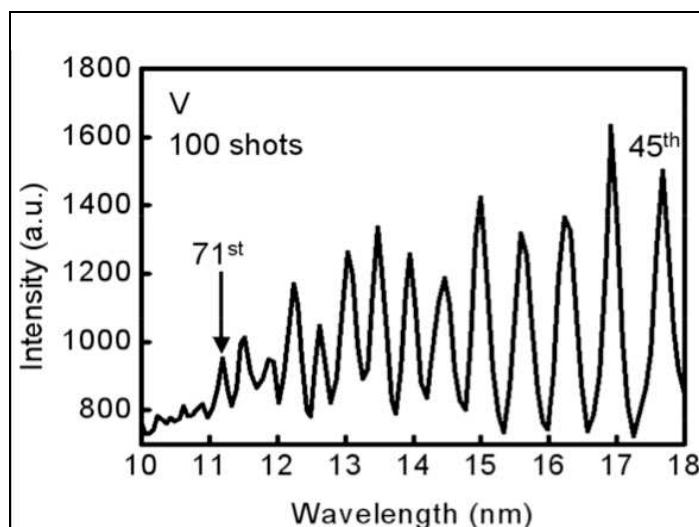

Fig. 3. HHG from the laser ablation vanadium plume, with a cut-off at the 71st harmonic (11.20 nm wavelength).

We attribute the observation of the vanadium cut-off at the 71st harmonic to contribution from doubly charged ions to the harmonic spectrum. The third ionization potential of vanadium is 29.31 eV, which is higher than the second ionization potential of boron. Therefore, harmonic generation from doubly- ionized vanadium will allow a cut-off higher than those from boron plasma. To investigate the nature of HHG from doubly charged ions in other ablation plumes, we have also measured the harmonic spectra generated from niobium, titanium, lead, and germanium. Table 1 shows the experimentally observed cut-off energy of HHG from laser plasma of niobium, titanium, vanadium, lead, and germanium plumes, generated by femtosecond laser pulses. The second ionization potentials of niobium, titanium, vanadium, lead, and germanium are 14.32, 13.58, 14.65, 15.03, and 15.93 eV, respectively. Furthermore, the third ionization potentials of these materials are 25.04, 27.49, 29.31, 31.94, and 34.22 eV, respectively. In the experiments, niobium, titanium, and vanadium showed relatively high cut-off energies of 76.42, 95.14, and 110.7 eV, respectively.

	Nb	Ti	V	Pb	Ge
Maximum cut-off energy (eV)	76.42	95.14	110.7	54.59	38.99
Second ionization (eV)	14.32	13.58	14.65	15.03	15.93
Third ionization (eV)	25.04	27.49	29.31	31.94	34.22

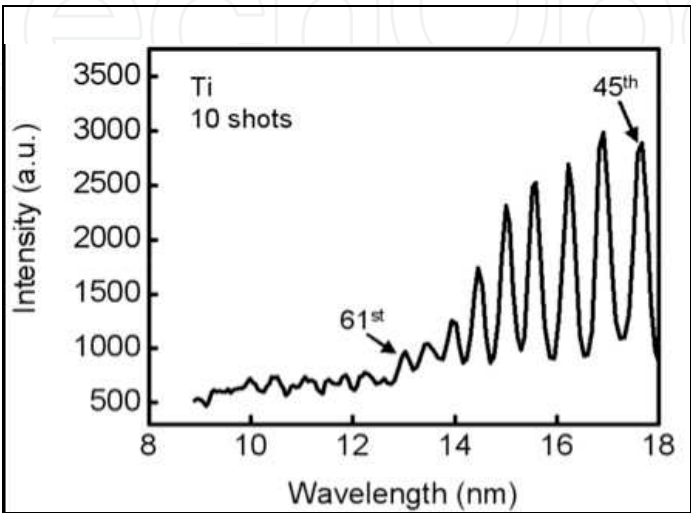Table 1. The harmonic cut-off energy and ionization potentials for Nb, Ti, V, Pb, and Ge atoms.

Fig. 4. HHG spectrum from laser ablation titanium plume, showing a cut-off at the 61st harmonic (13.03 nm wavelength).

Interestingly, however, the maximum cut-off energy of lead and germanium were limited to 54.59 and 38.99 eV, respectively. For example, the 61st harmonic (13.03 nm wavelength, 95eV photon energy) from the laser ablation titanium plume have been obtained as can be seen in Fig. 4. This is contrary to our hypothesis that higher ionization potentials generally yield higher cut-off harmonics, since, for example, the second and third ionization potentials of germanium are higher than vanadium, but the cut-off energy of germanium is only one-third of vanadium. The above results show that simple comparison of ionization potentials alone cannot definitively predict the relative cut-off harmonics among different atomic species. From our comparison with boron ablation, we can safely say that the HHG from the laser ablation niobium, titanium and vanadium were generated from doubly charged ions. Therefore, the relatively low cut-off from lead and germanium ablation can be attributed to the smaller contribution of harmonics from doubly charged ions. In these experimental conditions, the laser ablation plumes were not optimized for the lead and germanium target. As a result, self-defocusing of the femtosecond pump laser occurred from the electron by the leading edge of femtosecond laser pulse and the focusing intensity is decreased. Fig. 5 shows the maximum cut-off energy as a function of the ionization potential of the laser ablation plume used for nonlinear medium. Lead, zinc, indium, gold, silver, boron, titanium, and vanadium were used as the nonlinear medium in this experiment. The maximum cut-off energy has been increased when the ionization potential of the nonlinear medium increased. From Fig. 5, we can clearly see a good correlation between the cut-off energy and the ionization potential of the target material. This relatively clear correlation is also due to the fact that there is a maximum pump laser intensity that the ion can interact

with, before it further ionizes. Usually, this maximum intensity can be approximated by the barrier suppression intensity I_{BSI}, where I_{BSI} [eV] $\sim 4 \times 10^9$ $(I_P)^4/ Z_i^2$. Therefore, the maximum pump intensity (and as such U_P) is also a function of the ionization potential, and thus resulting in the strong correlation between the cut-off energy and I_P.
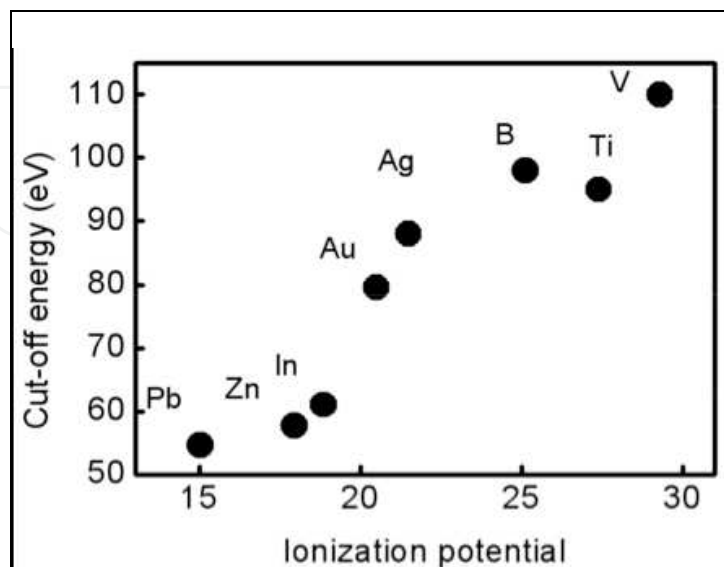

Fig. 5. The maximum observed cut-off energy as a function of the ionization potential of the nonlinear medium.

4. Intensity enhancement of single harmonic

Interesting results have been observed when the laser ablation of tin and indium plasma is used for harmonic generation. Fig. 6 shows the spectra of HHG from tin plasma pumped by femtosecond laser pulse. Plateau and cut-off of the harmonics have both been observed in these experiments. Although the signal is weak, high-order harmonics up to the 23rd order (34.56 nm wavelength) was observed with tin. However, the 17th order harmonic (at a wavelength of 46.76 nm) was unusually strong using tin laser ablation plume, as shown in Fig. 6 (Suzuki et al., 2006). The intensity of the 17th harmonics was 20 times higher than those of its neighbors. The conversion efficiency of the 17th harmonic was measured to be about 1.1×10^{-4}, and this output energy of 1.1 μJ was obtained from the pump laser energy of 10 mJ. To confirm the nature of this strong emission at the wavelength of 46.76 nm, we investigated the effect of the pump laser polarization on HHG. Fig. 7 shows the intensity of the 46.76 nm harmonic as a function of the laser polarization ellipticity. A quarter-wave plate was installed after the focusing lens to change the pump laser polarization from the linear to circular. The line intensities shown in Fig. 7 are normalized to that generated using linearly polarized pump laser, corresponding to the zero position. The intensity of emission at the wavelength of 46.76 nm decreased after 10-degree rotation of the quarter-wave plate, which completely disappeared after 50-degree rotation of the quarter-wave plate. This tendency is consistent with that of gas harmonics, which leads us to conclude that the strong emission at 46.76 nm should be generated by HHG. To investigate the mechanism of enhancement for the 17th harmonic, the central wavelength of the pump laser pulse was changed from 795 nm to 778 nm. Fig. 8 shows the HHG spectra from the laser-ablated tin with three different laser wavelengths of 795 nm, 782nm, and 778 nm (Suzuki et al., 2006).
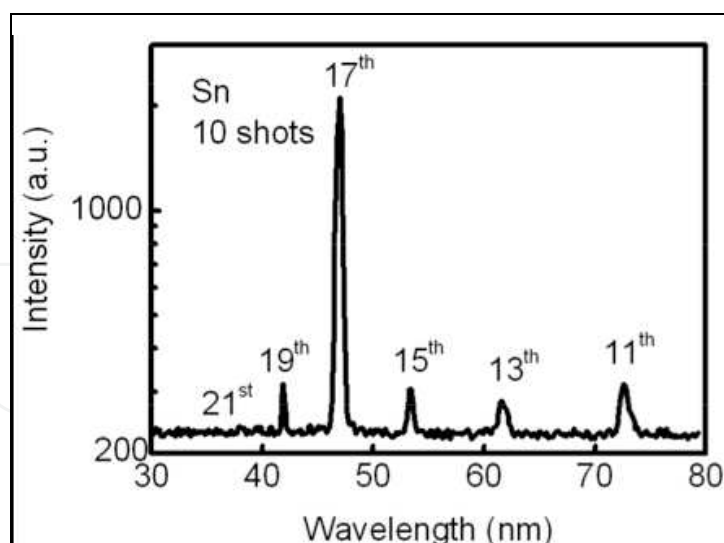
Fig. 6. HHG spectra from tin laser ablation irradiated by femtosecond laser pulse. Strong 17th harmonic (46.76 nm wavelength) is observed. (Suzuki et al., 2006)
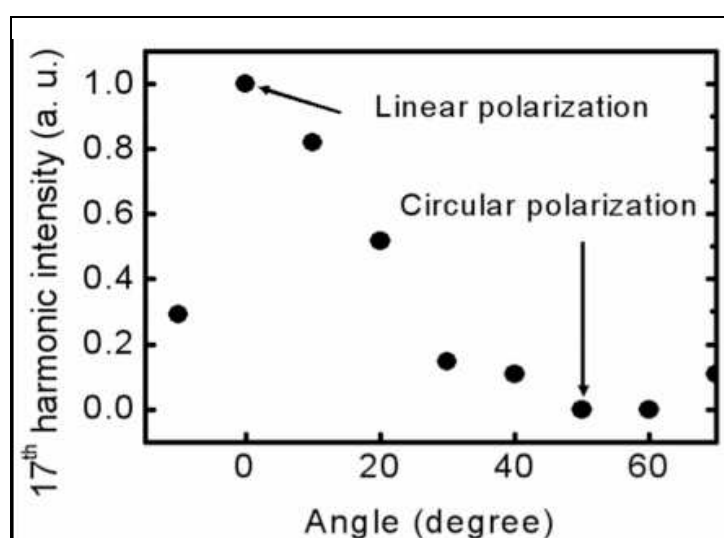

Fig. 7. Intensity of the 17th harmonic (46.76 nm wavelength) as a function of the quarter waveplate angle. The laser polarization is varied from linear (0 degree) to circular (45 degree). (Suzuki et al., 2006)

In Fig. 8(a), one sees that the intensity of the 17th harmonic using 795 nm wavelength pump dominates the harmonic spectrum. The intensity of the 17th harmonic is 20 times higher than that of other harmonics. However, in Fig 8(b), the intensity of the 17th harmonic using 782 nm wavelength pump is decreased, and is almost the same as that of other harmonics. In Fig. 8(c), the intensity of the 17th harmonic with 778 nm wavelength pump is further decreased. In this case, the 17th harmonic intensity is weaker than that of the 13th and 11th harmonics. The above results show that the intensity of the 17th harmonic gradually decreased as the wavelength of the pump laser become shorter. In past work, the Sn II ion has been shown to posses a strong transition of the $4d^{10}5s^25p$ $^2P_{3/2}$ - $4d^95s^25p^2$ (^1D) $^2D_{5/2}$ at the wavelength of 47.20 nm (Duffy & Dunne, 2001). The gf-value of this transition has been calculated to be 1.52 and this value is 5 times larger than other transition from ground state

of Sn II. Therefore, the enhancement of the 17th harmonic with 795 nm wavelength laser pulse can be explained be due to resonance with this transition. By changing the pump laser wavelength from 795 nm to 778 nm, the wavelength of the 17th harmonic is changed from 46.76 nm to 45.76 nm. Therefore, the wavelength of the 17th harmonic pumped by laser wavelength of 778 nm is farther away from the $4d^{10}5s^25p$ $^2P_{3/2}$ - $4d^95s^25p^2$ (^1D) $^2D_{5/2}$ transition, at the wavelength of 47.20 nm. As a result, the resonance condition of the 17th order harmonic is weaker when pumped by a 778 nm, compared with the case for 795 nm pump.
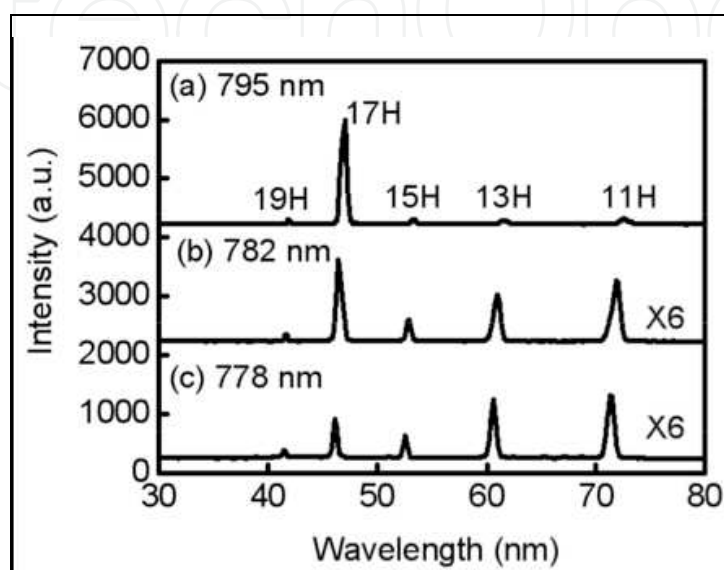

Fig. 8. HHG spectra from tin laser ablation for pump laser with central wavelength of (a) 795 nm, (b) 782 nm, and (c) 778 nm. The intensity of the spectra (b) and (c) are multiplied by 6 times. (Suzuki et al., 2006)

Fig. 9 shows the typical spectra of HHG from the laser ablation indium plume. In this experiment, the indium plasma was produced by a low-energy laser pulse, instead of the conventional gas medium. Exceptionally strong 13th harmonic at a wavelength of 61.26 nm have obtained as can be seen in Fig. 9. Using a 10 mJ energy Ti:sapphire laser pulse at a wavelength of 796.5 nm, the conversion efficiency of the 13th harmonic at a wavelength of 61 nm was about 8×10^{-5}, which was two orders of magnitude higher than its neighboring harmonics. The output energy of the 13th harmonic was measured to be 0.8 μJ. A cut-off of the 31st order at a wavelength of 25.69 nm has observed in this experiment.

For indium, the $4d^{10}5s^2$ $^1S_0$ - $4d^95s^25p$ (^2D) $^1P_1$ transition of In II, which has an absorption oscillator strength (gf–value) of 1.11 (Duffy et al., 2001)[30], can be driven in to resonance with the 13th order harmonic. Fig. 10 shows the HHG spectra at the wavelength of 796 and 782 nm. The intensity of the 13th harmonic for indium is attributed to such resonance of the harmonic wavelength with that of a strong radiative transition. By changing the laser wavelength from 796 nm to 782 nm, the 15th harmonic at the wavelength of 52.13 nm increased, and the intensity of the 13th harmonic decreased at the same time. The reason of the 15th harmonic enhancement is due to resonance with the $4d^{10}5s5p$ $^3P_2$ - $4d^95s5p^2$ (^2P) $^3F_3$ transition of In II, which has a gf-value of 0.30. The enhancement of the 15th order harmonic intensity is lower than that of the 13th harmonic because the gf-value of $4d^{10}5s5p$ $^3P_2$ - $4d^95s5p^2$ (^2P) $^3F_3$ transition is lower than that of the $4d^{10}5s^2$ $^1S_0$ - $4d^95s^25p$ (^2D) $^1P_1$ transition.

Furthermore the central wavelength of the 13th harmonic was driven away from resonance with the $4d^{10}5s^2$ $^1S_0$ - $4d^95s^25p$ (^2D) $^1P_1$ transition when using 782 nm wavelength laser, thereby decreasing the 13th order harmonics.
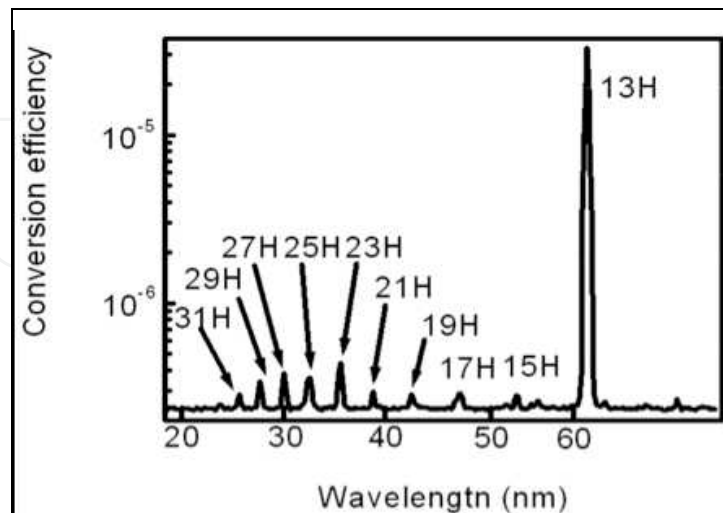

Fig. 9. Spectrum of the HHG from the laser ablation indium plume. The conversion efficiency is 8×10^{-5}.
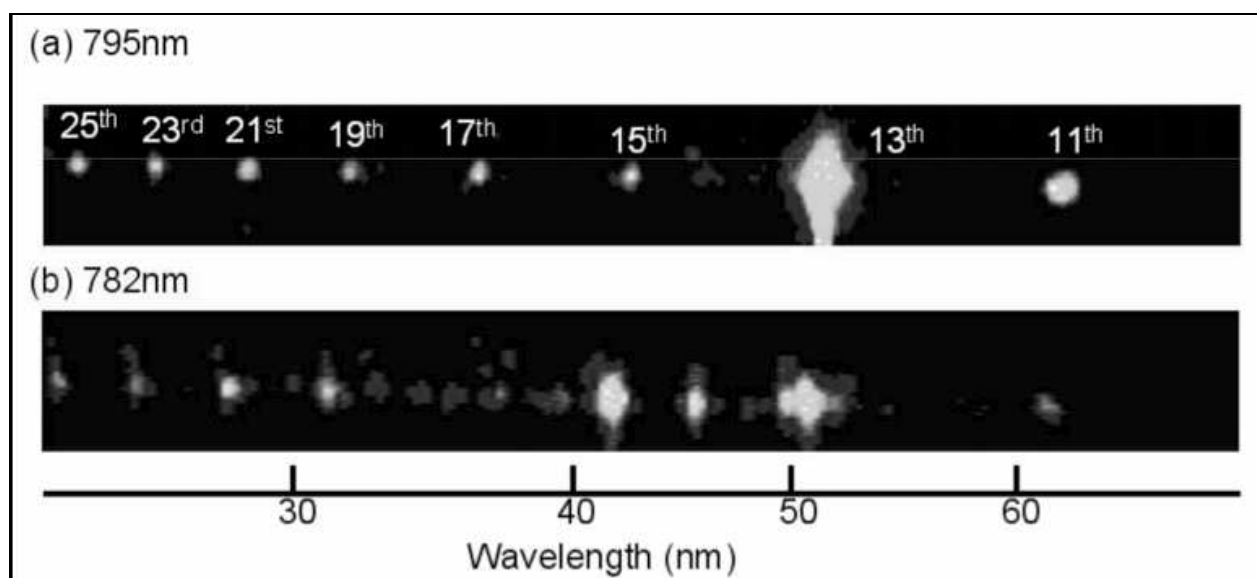

Fig. 10. HHG spectra from indium laser ablation for pump laser with central wavelength of (a) 795 nm, (b) 782 nm. The intensity of the 13th harmonic is two orders of magnitude higher than its neighboring harmonics.

There have been several discussions on the reason for this intensity enhancement of a single harmonic order. Taïeb et al. (Taieb et al., 2003a) have shown theoretically that if there is resonance between a specific harmonic order and a radiative transition, then considerable population could result on the upper state of the transition. Since electrons that ionizes from this excited state has a non-zero initial velocity, the electron driven by the laser electric field could recollide multiple times with the parent atom, thus increasing the harmonic emission. There is also work that explains the phenomenon to a better phase matching condition

under the presence of a strong radiative transition (Elouga-Bom et al., 2008). A strong absorption line will greatly modify the index of refraction near its wavelength. Under appropriate conditions, this could greatly improve the coherence length of a harmonic order close to this absorption, thus greatly increasing the intensity of this harmonic. Simulations using the actual parameters for indium plasma have shown that this theory explains well the intense 13th harmonic of indium.

5. High-order harmonics from nanostructured material

5.1 Silver nanoparticles

First, we performed harmonic generation experiments using silver nanoparticles glued on various substrates. We observed the nanoparticles used in this experiment with a scanning tunneling microscope, and we confirmed that their size varied between 90 to 110 nm. We initially verified that harmonics generated from the substrates themselves (glue, tape and glass) without the nanoparticles, was negligible compared with those from silver plasma. We fabricated the target so that a slab silver target was next to the nanoparticle target, with the two target surfaces at the same height. This target was placed on to the target holder, so that they interacted with both the prepulse and main pump laser at the same intensities. First, the prepulse and main pulse was aligned using a solid silver target, to search for conditions for maximum harmonic intensity within the plateau. Next, the target was translated so that the prepulse beam now irradiates the Ag nanoparticle target.
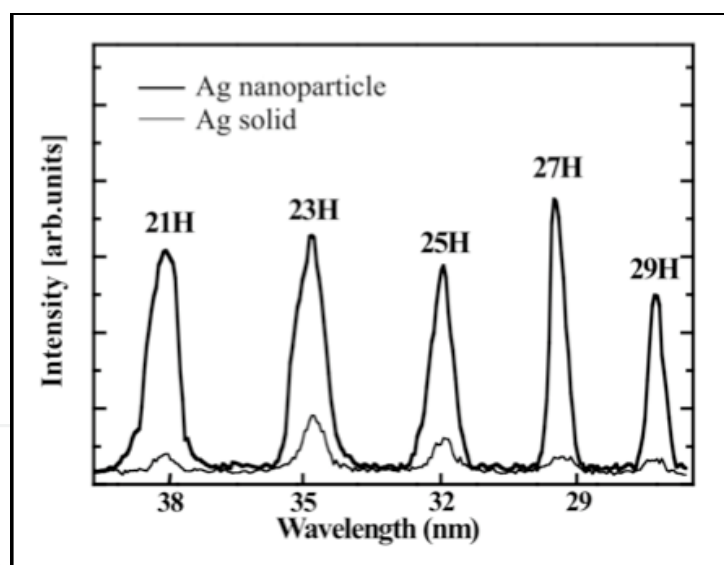

Fig. 11. Harmonic distribution in mid-plateau region for produced from bulk Ag target (thin lineout) and Ag nanoparticle plasma (thick lineout).

We compared the harmonic yield for silver nanoparticle targets with those from bulk silver targets, under the same prepulse and main pulse conditions. Fig. 11 shows the lineout of the harmonic spectra between the 21st and the 29th harmonics within the plateau. One clearly sees that the HHG intensity from the nanoparticle target was more than six times higher compared with that from bulk silver target. We can estimate the energy of these harmonics based on calibrations we have performed using longer (130 fs) pulses (Ganeev et al., 2005a). For 130 fs pump lasers, we have measured a conversion efficiency of 8×10⁻⁶ for bulk silver target. This would be a conservative estimate of the conversion efficiency for bulk silver

targets in the present work, which uses shorter 35 fs pulses. We therefore estimate a minimum harmonic conversion efficiency of 4×10^{-5} from silver nanoparticles within the plateau region. For the maximum main pump laser energy of 25 mJ used, the energy of the 21st to the 29th harmonics is evaluated to be more than 1 μJ.

When we compare the cut-off observed for harmonics from nanoparticle and slab silver targets, we also noted a slight extension of the harmonic cut-off for nanoparticles (Fig. 12). Harmonics up to the 67th order (103 eV photon energy) was observed in these studies with silver nanoparticles, while, for bulk silver target, the cut-off was at the 61st order (94 eV photon energy) under the same conditions. This slight extension of harmonic cut-off agrees with past observations, which noted similar extension in the cut-off for argon clusters, compared with isolated atoms (Donnelly et al., 1996)[19]. This difference has been explained by the increase in the effective binding energy of electrons in the cluster. The higher binding energy will allow the cluster to interact with laser intensities that are much higher than for isolated atoms, resulting in the extended cut-off for the former. In past works with Ar (Donnelly et al., 1996), the cut-off for clusters was at the 33rd order, compared with the 29th order cut-off for monomer harmonics.
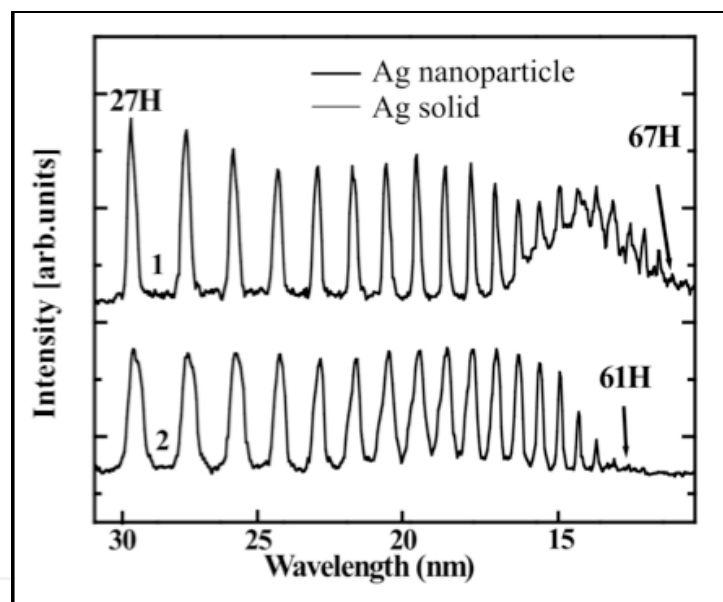

Fig. 12. High-order harmonic spectra generated from (1) silver nanoparticle plasma, and (2) plasma produced from bulk silver target.

Next, we studied the dependence of the harmonic yield on the pump intensity. However, the measurement was made difficult by the rapid shot-to-shot change in the harmonic intensity from Ag nanoparticle target. For experiments with solid slab targets, stable harmonic generation can be obtained for about ten minutes at 10 Hz repetition rates, without translating for a new target surface. However, for nanoparticle targets, the harmonics were strong for the first few shots, which were followed by a rapid decrease in harmonic yield when the plasma was created at the same target position. We attribute this effect to evaporation of the thin layer of nanoparticles. The first shot results in a strong harmonic spectrum, with the typical plateau-like structure starting from the 17th order. Then, for the second and third shots, the intensity of the harmonics decreased drastically, and, for the fourth shot and after, the harmonics almost disappeared. We repeated the

experiments with nanoparticles many times, revealing the same feature. We also observed that, when we used different material as the substrate, there was a different behavior of the shot-to-shot decrease in harmonic yield. Another interesting feature found in the experiments with nanoparticle targets was that the prepulse intensity necessary for HHG was lower than that used for bulk targets.

These observations give us a rough picture of the ablation for nanoparticle targets. The material directly surrounding the nanoparticles is polymer (epoxy glue), which has a lower ablation threshold than metallic materials. Therefore, the polymer starts to ablate at relatively low intensities, carrying the nanoparticle with it, resulting in the lower prepulse intensity. Polymer also has a lower melting temperature than metals. Therefore, repetitive irradiation of the target leads to melting and change in the properties of the target. This results in the change in conditions of the plasma plume, resulting in a rapid decrease in the harmonic intensity with increased shots. The different shot-to-shot harmonic intensities for different substrates can be explained by the different adhesion properties of nanoparticles to the substrate.

Due to such rapid change in the conditions for harmonic generation with nanoparticle targets, it was difficult to define precisely the dependence of harmonic yield on prepulse and main pulse intensities. Nevertheless, approximate measurements of the dependence of harmonic yield on the main pulse intensity for Ag nanoparticles have shown a saturation of this process at relatively moderate intensities ($I_{fp} \approx 8 \times 10^{14}$ W cm^{-2}).

Harmonics from plasma nanoparticles also displayed several characteristics similar to gas harmonics. First, the harmonic intensity decreased exponentially for the lower orders, followed by a plateau, and finally a cut-off. Next, the harmonic intensity was strongly influenced by the focus position of the main pump laser, along the direction parallel to the harmonic emission. The strongest harmonic yield was obtained when the main pump laser was focused 4 to 5 mm after the nonlinear medium. We observed the same tendency of the harmonics using bulk silver target. The typical intensity of the pump laser for maximum harmonic yield was between 5×10^{14} to 2×10^{15} W cm^{-2}. These results agree with those of gas harmonics (Lindner et al., 2003), and are due to the selective short-trajectory-generated harmonics when the pump laser is focused after the medium. Harmonics from short-trajectories have a flat and large area on-axis, with excellent phase matching conditions, resulting in the higher harmonic yield. In our case, we needed to focus the pump laser away from the medium, since the total intensity that would be produced at focus would exceed the barrier suppression intensity for multiply charged ions. This would result in over-ionization of the plasma, leading to the decrease in the harmonic yield.

To study the size effect of nanoparticles, we performed harmonic generation experiments using colloidal silver targets, which are contains blocks of silver with sizes between 100 to 1000 nm. We confirmed the size of the silver blocks by viewing with a scanning tunneling microscope. The results showed that the harmonic yield for these sub-μm-sized silver blocks was much lower than that from nanoparticles, and was comparable to those from bulk silver targets. We also noted a tendency of slightly extended harmonic cut-off for smaller particle sizes. The cut-offs for the harmonics were at the 61st, 63rd and 67th order, for bulk silver, sub-μm silver colloid and silver nanoparticle targets, respectively.

These studies have shown that the increasing the particle size over some limit is undesirable due to the disappearance of enhancement-inducing processes. The observed enhancement of

harmonic yield for plasma plume with 90 to 110 nm size nanoparticles can probably be further improved by using smaller nanoparticles.

These experiments show that the size of the nanoparticles is of essential importance for harmonic generation. To gain maximum HHG conversion efficiency, it is essential to know the maximum tolerable particle size for increased harmonic yield. On one hand, increasing the size of the particles increases its polarizability, and large polarizability of a medium is critical for efficient harmonic generation (Liang et al., 1994). On the other hand, the increase in particle size leads to phenomena that reduces harmonic yield (such as HHG only from surface atoms (Toma et al., 1999), and reabsorption of harmonics).

The increased HHG efficiency for silver nanoparticles might also be an important factor for explaining the high conversion efficiency of HHG from plasma produced from bulk silver targets. Silver has been known to be a highly efficient material for plasma HHG, but up to now the reason was not clear (Taieb et al., 2003a). However, it is known that nanoclusters (such as Ag_2 and Ag_8) and nanoparticles are abundantly produced by laser ablation. Since our laser plume expanded adiabatically for 100 ns before irradiation by the main pulse, one can expect that the silver plume from bulk silver target also contained many nanomaterials, which would contribute to increasing the HHG efficiency.

5.2 Other nanoparticles

To study what parameters affect the strong harmonics from nanoparticles, we next performed experiments using nanoparticles of different materials. An example of the harmonic spectrum from chromium oxide (Cr_2O_3) nanoparticle target is shown in Fig. 13(a). The spectrum from nanoparticle targets showed a featureless plateau with a cut-off at the 31st harmonic, with harmonic yield that is much stronger than those from bulk Cr_2O_3 targets (Fig. 13(b)). Another important observation is that the relative intensities between harmonic orders differ for different targets. For nanoparticle targets, the harmonic spectrum resembles those observed from gas, with a plateau followed by a cut-off. However, harmonics from bulk Cr_2O_3 target has a characteristic enhancement of the 29th order, and a cut-off at the 35th harmonic, which has also been observed in previous studies of HHG in chromium plasma (Ganeev et al., 2005c)[24]. For bulk chromium oxide targets, the 29th harmonic is about 10 times stronger than the lower 27th harmonic. Such enhancement was not observed with Cr_2O_3 nanoparticle targets at moderate prepulse intensities (5×10^9 W cm-2). We should note that by further increasing the prepulse intensity to 9×10^9 W cm-2, we could generate intense 29th harmonic from Cr_2O_3 nanoparticle targets. This is a sign of ionization of the nanoparticles in the plasma, since enhanced single harmonic in chromium has previously been attributed to the proximity of the 29th harmonic with the giant 3p - 3d ionic transitions of singly ionized chromium ions (Ganeev et al., 2005c). The delay between the prepulse and main pulse in these experiments was kept at 25 ns.

High-order harmonics from other nanoparticles also showed similar features, with a notable enhancement of low-order harmonics at the plateau and a decrease in the harmonic cut-off compared with harmonics using bulk targets. For example, Fig. 13(c) and (d) show the harmonic spectrum for manganese titanium oxide ($MnTiO_3$) nanoparticles and bulk targets, respectively. The $MnTiO_3$ nanoparticles show relatively strong 19th and 21st harmonics, with a cut-off at the 25th order, whereas the bulk MnTiO3 targets show only weak harmonics that are comparable to noise. Increasing the femtosecond pump intensity did not lead to extension of the harmonic cut-off for nanoparticle targets, which is a sign of saturation of the

HHG in these media. Also, at relatively high femtosecond pump intensities, we noted a decrease in the harmonic conversion efficiency due to the onset of negative effects (such as increase in the free electron density, self-defocusing and phase mismatch). Similar effects were also observed when we increased the prepulse intensity, which is attributed to the increase in the free electron density of the plasma, resulting in phase mismatch.
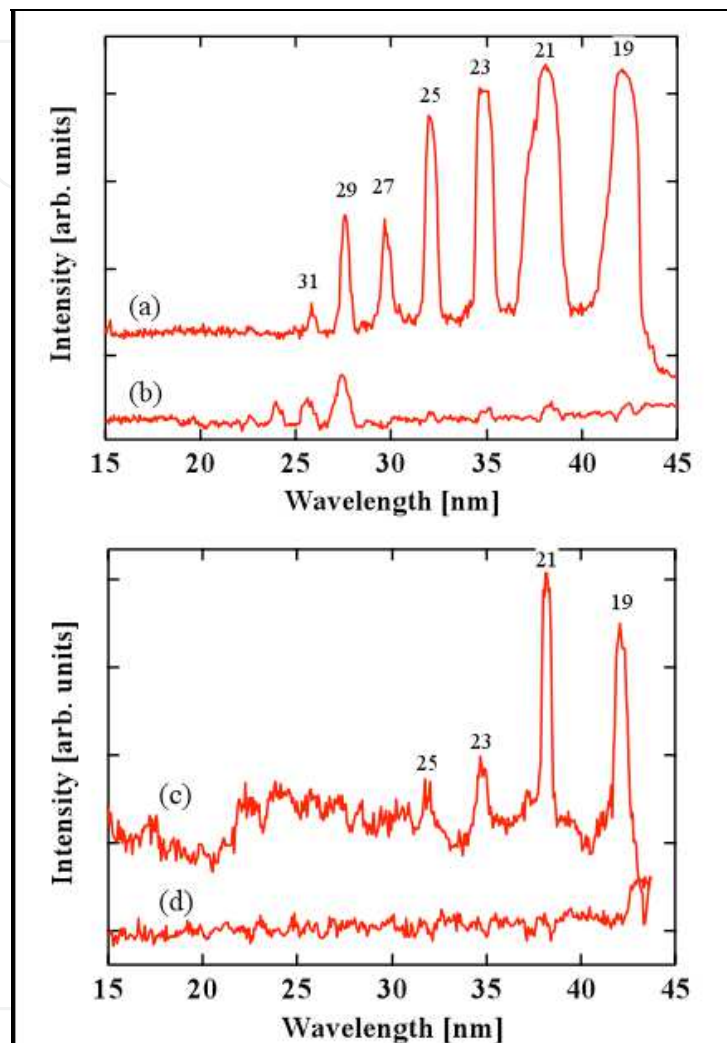

Fig. 13. Harmonic spectrum for (a) chromium oxide nanoparticles, (b) chromium oxide bulk, (c) manganese titanium oxide nanoparticles, and (d) manganese titanium oxide bulk targets.

A comparison of the low-order harmonic generation using the single atoms and multiparticle aggregates has previously been reported for Ar atoms and clusters (Donnelly et al., 1996)[7]. It was demonstrated that a medium of intermediate-sized clusters with a few thousand atoms of an inert gas has a higher efficiency for generating the harmonics, compared with a medium of isolated gas atoms of the same density. The reported enhancement factor for the 3rd to 9th harmonics from gas jets was about 5. In our HHG experiments with the laser-ablated nanoparticles, these observations were extended toward the higher-order harmonics and stronger enhancement for the harmonics up to the 25th order was achieved. These results have also shown that the dependence of the HHG efficiency on the prepulse and main pulse intensity is much more prominent for nanoparticles than for monatomic particles.

Since nanoparticles are smaller than the laser wavelength, they contain many equivalent, optically active electrons at effectively the same point in the laser field. This leads to the possibility that each of these electron oscillators may contribute coherently to a global nanoparticle dipole. However, this statement is true only for low-order harmonics. For high-order harmonic generation (such as those considered in this paper), the dipole approximation is inapplicable, because the harmonic radiation wavelength is shorter than the size of nanoparticles (about 100 nm).

We would like to point out that in our experiments with nanoparticles, the intense harmonics were observed (i) only for lower orders, (ii) when the intensity of the picosecond prepulse (which generates the plasma plume) was moderate. When the prepulse intensity was increased, phenomena that are explained by the presence of ions appeared. For example, enhancement of the 29th harmonic in chromium is related to the giant 3p - 3d ionic transitions of Cr^+, which started to appear for Cr_2O_3 nanoparticles when the prepulse intensity was increased to 9×10^9 W cm^{-2}. These results suggest that one major reason for the intense harmonics from nanoparticles is the contribution from neutral atoms. Since neutral atoms are larger compared with its ions, the recombination probability of the electron wave packet that was liberated by the laser electric field is also larger for neutral atoms. As a result, the neutral atoms emit stronger harmonics than ions, but with a lower cut-off due to its lower ionization potential.

5.3 C_{60} fullerenes
5.3.1 Harmonic generation from C_{60} fullerenes

A problem with experiments using nanoparticles is that there is always a distribution in their size and shape. Since phenomena such as ionization and nonlinear response to intense laser fields should vary with nanoparticle dimensions, it becomes difficult to determine how the various characteristics of the nanostructured material affect harmonic generation. To study HHG from a more uniform nano-material, we decided to next explore C_{60} fullerenes. In our previous experiments, we demonstrated HHG from laser-produced plasma of fullerene targets (Ganeev et al., 2009). In that work, we showed that (i) the harmonics lying within the spectral range of SPR in C_{60} (20 - 22 eV) are enhanced, (ii) the harmonic efficiency from C_{60} targets are 20 to 25 times larger for the 13th harmonic compared with those generated from carbon monomer rich plasma, and (iii) the harmonic cut-off in C_{60} is lower (19th order) than carbon but extends beyond the value (11th order) predicted by the three-step model. Here, we present a more detailed account of HHG from C_{60} fullerenes.

Fig. 6 shows the harmonic spectra from C_{60} for different delays between the pump pulse and the femtosecond driving pulse. HHG by ablation of bulk materials is influenced by the temporal delay between the pump pulse and driving pulse, as it results in a change in the atomic density and plasma length of the nonlinear medium. To study their effects on the harmonic intensity, we varied the delay from 18 ns to 100 ns. Our measurements showed no significant changes in the harmonic intensities in C_{60} (see Fig. 13(a) and (b)) for delays of 22 ns and 63 ns, with some two-fold increase of harmonic efficiency for the shorter delay. By comparing with calibrated harmonics from silver plasma (Ganeev, 2007), we estimate the efficiency of the 13th harmonic from fullerene plasma to be near 10-4.

However, for bulk targets such as C, Cr and Mn, no harmonics were observed from plasmas when we used the shorter delays, which is contrary to the case of C_{60}. This can be attributed to the non-optimal plasma conditions, since it requires time for the plasma to ablate on the

bulk surface and expand into the area where the femtosecond beam interacts with the plasma. This can also be inferred from the lower pump pulse intensity ($I_{pp} \sim 2 \times 10^9$ W cm^{-2}) needed for HHG from C_{60}-rich target, compared with that needed for bulk targets [Ipp > 10^{10} W cm^{-2}]. We believe that short delays lead to more favorable evaporation conditions and higher particle density for the cluster-rich medium compared with the monatomic medium, thus resulting in a higher harmonic yield. Usually for heavy bulk targets, the strong harmonics were observed using longer delays (40-70 ns). The use of light targets (B, Be, Li) showed an opposite tendency, where one can obtain effective HHG for shorter delays. The optimization is related to the presence of a proper density of particles within the volume where harmonics are generated, which depends on the propagation velocity of the plasma front. For C_{60}, one can expect to optimize HHG at longer delays due to the larger weight of the fullerene particles. However, one also needs to take into account the possibility of the presence of the fragments of C_{60} in the plume, in which case, the density of the medium within the laser-interaction region becomes sufficient even for shorter delays.
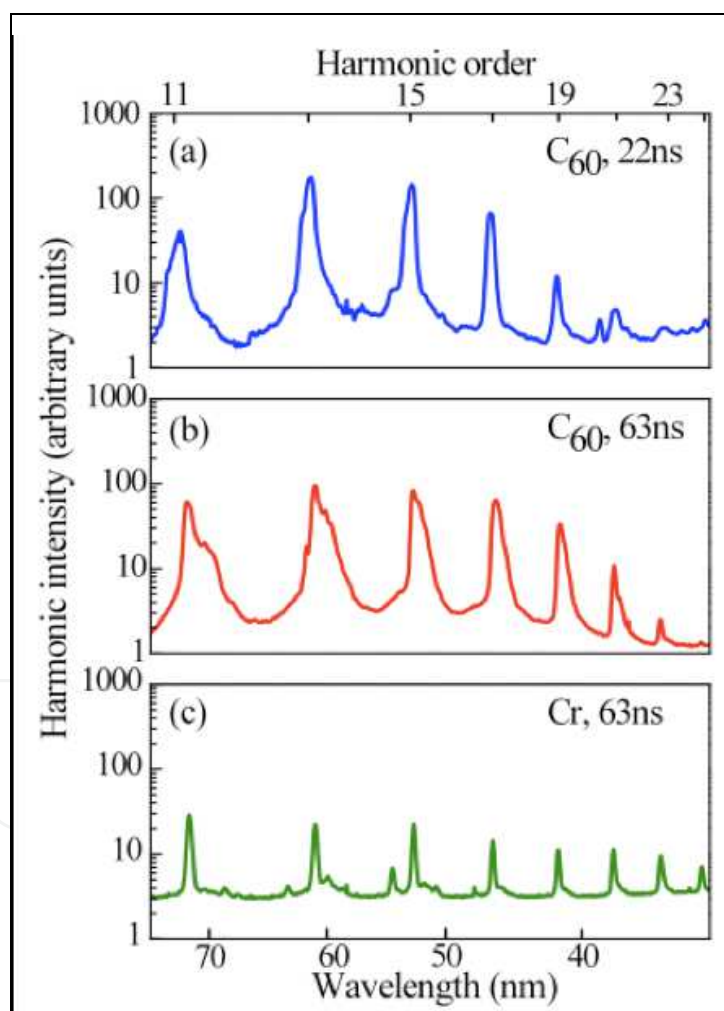

Fig. 13. Harmonic generation observed in C_{60} plasma at (a) 22 ns and (b) 63 ns delays between the prepulse and main pulse and (c) in chromium plasma

An interesting feature of the fullerene harmonic spectra is that the spectral width is about three to four times broader compared with those generated in plasma rich with monatomic particles (1.2 nm and 0.3 nm FWHM, respectively). For comparison, Fig. 13(c) shows the

harmonic spectra for Cr bulk targets. Broader width of the harmonics can be explained by self-phase modulation and chirping of the fundamental radiation propagating through the fullerene plasma. Broadening of the main beam bandwidth causes the broadening of the harmonic's bandwidth. Increase in the harmonic bandwidth with delay can be explained by the longer length of the fullerene plasma for the longer delay, and thus stronger self-phase modulation of the femtosecond pump laser.

The intensities of the pump pulse and driving pulse are crucial for optimizing the HHG from C_{60}. Increasing the intensity of the driving pulse did not lead to an extension of the cut-off for the fullerene plasma, which is a sign of HHG saturation in the medium. Moreover, at relatively high femtosecond laser intensities, we observed a decrease in the harmonic output, which can be ascribed to phase mismatch resulting from higher free electron density. We observe a similar phenomenon when the pump pulse intensity on the surface of fullerene-rich targets is increased above the optimal value for harmonic generation. This reduction in harmonic intensity can be attributed to phenomena such as the fragmentation of fullerenes, an increase in free electron density, and self-defocusing. At relatively strong ablation intensity for fullerene film (I_{pp} > 1×10^{10} W cm^{-2}), we observed only the plasma spectrum, without any sign of harmonics.

The stability of C_{60} molecules to ionization and fragmentation is of particular interest, especially for their application as a medium for HHG. The structural integrity of the fullerenes ablated off the surface should be intact until the driving pulse arrives. Therefore, the pump pulse intensity is a sensitive parameter. At lower intensities the density of clusters in the ablation plume would be low, while at higher intensities one can expect fragmentation. C60 has demonstrated both direct and delayed ionization and fragmentation processes and is known to survive even in intense laser fields. This can be attributed to the large number of internal degrees of freedom that leads to the fast diffusion of the excitation energy (Bhardwaj et al., 2003). At 796 nm, multiphoton ionization is the dominant mechanism leading to the ionization of C_{60} in a strong laser field. The collective motion of π electrons of C_{60} can be excited by multiphoton process. Since the laser frequency is much smaller than the resonance frequency of π electrons, barrier suppression and multiphoton ionization are the dominant mechanisms leading to the ionization in a strong laser field.

Another important parameter that affects the stability of HHG process is the thickness of the fullerene target. We obtained stable harmonic generation with low shot-to-shot variation in harmonic intensity by moving the fullerene film deposited on the glass substrate after several laser shots. This avoids decrease in the fullerene density due to ablation of the thin film. The number of laser shots at the same target position that resulted in stable harmonic emission decreased drastically with the film thickness. For example, in a 10- μm film, the harmonic emission disappeared after 70 to 90 shots, whereas in a 2-μm film, the harmonics disappeared after 5 to 7 shots.

To understand the origin of the harmonic emission in C_{60}, we studied its dependence on the polarization of the main pulse. This also allows one to distinguish the plasma emission from the HHG. HHG is highly sensitive to laser polarization, since the trajectories of the recolliding electrons are altered significantly for elliptically polarized pump lasers, thus inhibiting the recombination process. We noted that the harmonic signal drop rapidly and disappear with ellipticity of the laser polarization. For circular polarization, as expected, the harmonic emission disappears and the resulting background spectrum corresponds to the plasma emission.

Does the influence of plasmon resonance on the HHG in fullerene plasma depend on the wavelength of the driving field? To address this question, we also studied HHG using the second harmonic (396 nm, 4 mJ, 35 fs) of the main pulse (793 nm, 30 mJ). The low second harmonic conversion efficiency did not allow us to achieve the laser intensities reached with the 793 nm fundamental laser. As a result, we were able to generate harmonics up to the 9th order of the 396 nm driving pulse, while simultaneously generating harmonics using the 793 nm laser. Harmonic generation using two main pulses (793 nm and 396 nm) did not interfere with each other, due to different focal positions of these two beams (~2 mm in the Z-axis and ~0.2 mm in the X-axis). Therefore, the two HHG processes occurred in different regions of the laser plasma. Here, the Z-axis is the axis of propagation of the driving beam, and the X-axis is the axis vertical to the Z-axis. This axis is defined by the walk-off direction of the second harmonic with respect to the fundamental driving pulse.
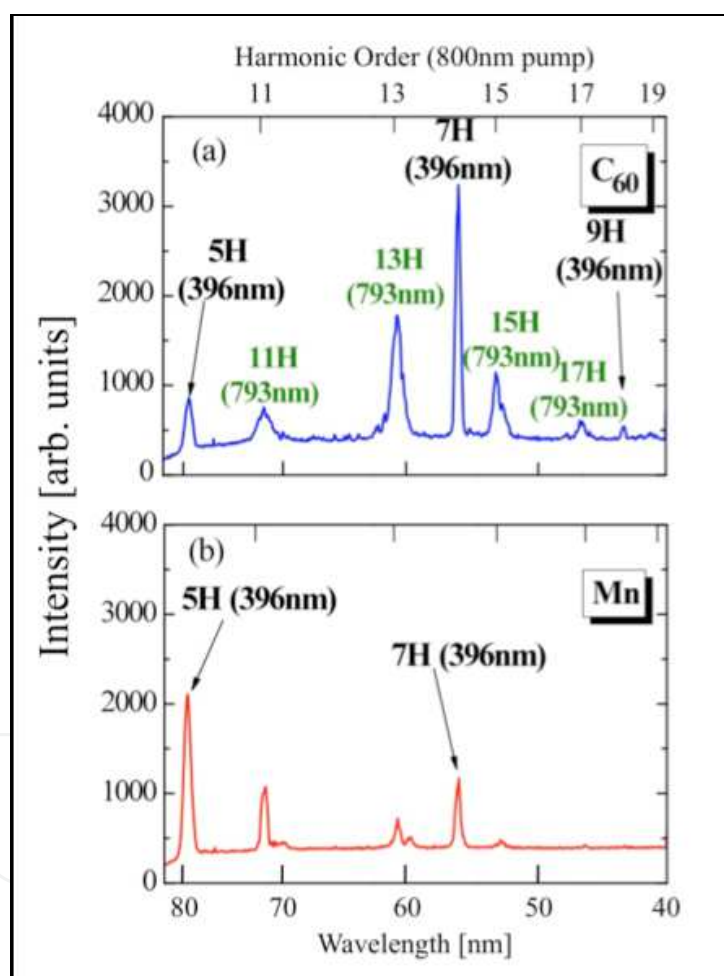

Fig. 14. Harmonic spectra from (a) C_{60} and (b) Mn plasma, when both the 793 nm and 396 nm laser were simultaneously focused on the laser-produced plasma.

Fig. 14(a) shows the HHG spectrum from C_{60} fullerene optimized for the second harmonic driving pulse. The energy of the second harmonic is ~1/7th of the fundamental. One can see the enhancement of the 7th harmonic (which is within the spectral range of the SPR of C_{60}) compared with the 5th harmonic. This behavior is similar to that observed for the 793 nm driving pulse. For comparison, we present in Fig. 14(b) the optimized harmonics generated

using the 396 nm pump and the weak harmonics from the 793 nm radiation in manganese plasma. One can see a decrease in harmonic intensity from the Mn plasma for each subsequent order, which is a common case, when one uses a nonlinear optical medium containing atomic or ionic particles. These studies confirmed that, independent of the driving pulse wavelength, the harmonics near SPR in C_{60} are enhanced.

5.3.2 Simulations of C_{60} harmonic spectra

To understand the influence of the absorptive properties of surface plasmon resonance on the harmonic emission spectrum in C_{60}, we simulated the emission spectrum using parameters that are roughly identical to those used in experiments. The HHG efficiency can be understood by three length parameters. For optimum HHG, the length of the nonlinear medium L_{med} should be (a) larger than the coherence length $L_{coh} = \pi/\Delta k$, which is defined by the phase mismatch between the fundamental and harmonic fields ($\Delta k = k_q - qk_0$ where k_q and k_0 are the harmonic and fundamental wave vectors, respectively) and depends on the density and ionization conditions, and (b) smaller than the absorption length of the medium $L_{abs} = 1/\rho\sigma$, where ρ is the atomic density and σ is the ionization cross-section.

The photoionization cross-section of C_{60} is well known, both experimentally and theoretically. It displays a giant and broad plasmon resonance at ~ 20 eV (around the 11th, 13th and 15th harmonics, with a bandwidth of 10 eV FWHM). We calculated the absorption length using the estimated fullerene density in the interaction region (5×10^{16} cm^{-3}) and the known photoionization cross-sections. The absorption length varies from 0.8 mm (for the 7th and 17th harmonic) to 0.3 mm (for the 11th, 13th and 15th harmonic), suggesting that harmonics near the plasmon resonance should be more strongly absorbed in the medium (whose length is estimated to be about 0.8 - 1 mm). Due to this increased absorption in C_{60}, we expect a dip in the harmonic spectrum for the 11th - 15th harmonics. Our calculations also point out that harmonics produced in bulk carbon target are not absorbed by the nonlinear medium. With an assumed medium length of 1 mm, theoretical spectra are obtained by using the proper wavelength-dependent index of refraction and dispersion data.
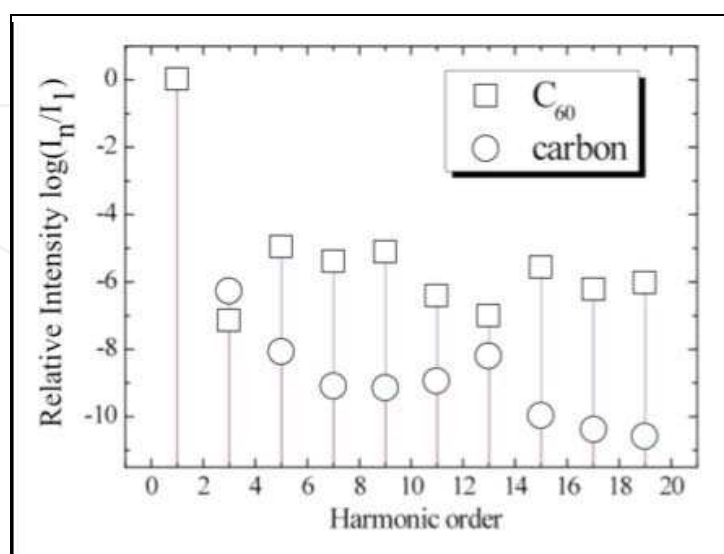

Fig. 15. Calculated relative intensities of harmonics generated from neutral carbon mono-atom and C_{60} fullerene molecule.

From our calculations, we find that for bulk carbon, the influence of absorption on the harmonic yield is negligible and as a result the overall harmonic spectrum is determined by dispersion. The harmonic yield decreases with increasing order as it becomes difficult to phase match higher orders. In C_{60}, absorption of harmonics by the nonlinear medium is dominant due to large photoabsorption cross-sections. The effect of dispersion only lowers the HHG efficiency but does not affect the overall shape of the spectrum. As a result, one expects the harmonic yield to decrease considerably near the surface plasmon resonance, if one does not consider the nonlinear optical influence of this resonance on the harmonic efficiency in this medium. On the contrary, in our experiment, we observed a notable enhancement of these harmonics in the fullerene-rich plume (Figs. 13 and 14). This is a signature of multi-electron dynamics in a complex molecule such as C_{60} and has no atomic analogue.

To understand the origin of enhancement of harmonic yield near SPR, we theoretically studied the interaction of monatomic carbon and fullerene C_{60} molecule with a strong laser pulse by the time–dependent density functional theory (TDDFT) (Runge & Gross, 1984). In the TDDFT approach, the many-body time-dependent wave-function is replaced by the time-dependent density, which is a simple function of the three-dimensional vector r. n(r,t) is obtained with the help of a fictitious system of non-interacting electrons by solving the time-dependent Kohn-Sham equations. These are one-particle equations, so it is possible to treat large systems such as fullerenes. For all calculations we used the OCTOPUS code (Marques et al., 2003) with norm-conserving non-local Troullier-Martins pseudopotentials (Troullier & Martins, 1991), Slater exchange, Perdew and Zunger correlation functionals (Perdew & Zunger, 1981) and grid spacing of 0.6 Å for parallelepiped box of 8×8×60 Å.

We analyzed the relative harmonic intensities calculated for C_{60} and bulk carbon (Fig. 8). A significant increase in HHG efficiency for C_{60} molecule can be attributed to additional oscillation of the time-dependent dipole in the C_{60} molecule. This can be a sign of an induced collective plasmon-like response of the molecule to external field. At the same time the cut-off for the carbon atom is higher than that for a fullerene molecule. Treating relatively high-order harmonics with our simulation codes can become inaccurate, due to an exponential cut-off of the exchange and correlation potential. The effects of correlation for lower harmonics are nevertheless conserved, so a collective oscillation can be responsible for the relative increase of the time-dependent dipole and, respectively, HHG conversion efficiency observed in plasma of fullerene molecules.

6. Conclusion

In this chapter, we have reviewed recent developments in the generation of intense high-order harmonics using lowly ionized plasma as the nonlinear medium. We have shown recent results that demonstrate clear plateau with a cut-off as high as the 101st order. A unique intensity enhancement of a single high-order harmonic that dominates the spectrum has been observed in the XUV region. Such enhancement of a single harmonic is an advantage for several important applications of coherent XUV radiation. One example is photoelectron spectroscopy for understanding excited-state electron dynamics, in which there is a need to select one harmonic while eliminating neighboring harmonics. This single enhancement technique will allow the generation of a quasi-monochromatic coherent x-ray source, without complexities of using monochromators, multilayer mirrors and filters. Another characteristic of this plasma harmonic method is that one could use any target that

could be fabricated into solids. Profiting from this feature, there has been several works on pioneering high-order harmonic generation from nanostructured material, such as metallic nanoparticles and fullerenes.

7. References

Akiyama, Y., Midorikawa, K., Matsunawa, Y., Nagata, Y., Obara, M., Tashiro, H. & Toyoda, K. (1992). Generation of high-order harmonics using laser-produced rare-gas-like ions *Phys. Rev. Lett.* 69, 2176-2179.

Bhardwaj, V., Corkum, P. & Rayner, D. (2003). Internal laser-induced dipole force at work in c-60 molecule *Phys Rev Lett* 91, 203004.

Constant, E., Garzella, D., Breger, P., Mevel, E., Dorrer, C., Le Blanc, C., Salin, F. & Agostini, P. (1999). Optimizing high harmonic generation in absorbing gases: Model and experiment *Physical Review Letters* 82, 1668-1671.

Corkum, P. (1993). Plasma perspective on strong-field multiphoton ionization *Phys. Rev. Lett.* 71, 1994-1997.

Donnelly, T., Ditmire, T., Neuman, K., Perry, M. & Falcone, R. (1996). High-order harmonic generation in atom clusters *Phys. Rev. Lett.* 76, 2472-2475.

Drescher, M., Hentschel, M., Kienberger, R., Tempea, G., Spielmann, C., Reider, G., Corkum, P. & Krausz, F. (2001). X-ray pulses approaching the attosecond frontier 291, 1923-1927.

Duffy, G. & Dunne, P. (2001). The photoabsorption spectrum of an indium laser produced plasma *J Phys B-At Mol Opt* 34, L173-L178.

Duffy, G., Van Kampen, P. & Dunne, P. (2001). 4d -> 5p transitions in the extreme ultraviolet photoabsorption spectra of snii and sniii *J Phys B-At Mol Opt* 34, 3171-3178.

Elouga-Bom, L.-B., Bouzid, F., Vidal, F., Kieffer, J.-C. & Ozaki, T. (2008). Correlation of plasma ion densities and phase matching with the intensities of strong single high-order harmonics *J Phys B-At Mol Opt* 41, 215401.

Faria, C. F. D., Kopold, R., Becker, W. & Rost, J. M. (2002). Resonant enhancements of high-order harmonic generation *Physical Review A* 65, -.

Gaarde, M. B. & Schafer, K. J. (2001). Enhancement of many high-order harmonics via a single multiphoton resonance *Physical Review A* 6401, -.

Ganeev, R., Baba, M., Suzuki, M. & Kuroda, H. (2005a). High-order harmonic generation from silver plasma *Physics Letters A* 339, 103-109.

Ganeev, R., Suzuki, M., Baba, M. & Kuroda, H. (2005b). Generation of strong coherent extreme ultraviolet radiation from the laser plasma produced on the surface of solid targets *Appl Phys B-Lasers O* 81, 1081-1089.

Ganeev, R., Suzuki, M., Baba, M. & Kuroda, H. (2005c). Harmonic generation from chromium plasma *Appl Phys Lett* 86, 131116.

Ganeev, R., Suzuki, M., Baba, M., Kuroda, H. & Ozaki, T. (2005d). High-order harmonic generation from boron plasma in the extreme-ultraviolet range *Optics Letters*.

Ganeev, R., Suzuki, M., Baba, M., Kuroda, H. & Ozaki, T. (2006). Strong resonance enhancement of a single harmonic generated in the extreme ultraviolet range *Optics Letters* 31, 1699-1701.

Ganeev, R. A. (2007). High-order harmonic generation in a laser plasma: A review of recent achievements *J Phys B-At Mol Opt* 40, R213-R253.

Ganeev, R. A., Bom, L. B. E., Abdul-Hadi, J., Wong, M. C. H., Brichta, J. P., Bhardwaj, V. R. & Ozaki, T. (2009). Higher-order harmonic generation from fullerene by means of the plasma harmonic method *Physical Review Letters* 102, 013903.

Ganeev, R. A., Bom, L. B. E., Kieffer, J.-C., Suzuki, M., Kuroda, H. & Ozaki, T. (2007). Demonstration of the 101st harmonic generated from a laser-produced manganese plasma *Phys Rev A* 76, 023831.

Goulielmakis, E., Schultze, M., Hofstetter, M., Yakovlev, V. S., Gagnon, J., Uiberacker, M., Aquila, A. L., Gullikson, E. M., Attwood, D. T., Kienberger, R., Krausz, F. & Kleineberg, U. (2008). Single-cycle nonlinear optics *Science* 320, 1614-1617.

Kazamias, S., Douillet, D., Weihe, F., Valentin, C., Rousse, A., Sebban, S., Grillon, G., Auge, F., Hulin, D. & Balcou, P. (2003). Global optimization of high harmonic generation *Phys. Rev. Lett.* 90, 193901.

Kim, I. J., Kim, C. M., Kim, H. T., Lee, G. H., Lee, Y. S., Park, J. Y., Cho, D. J. & Nam, C. H. (2005). Highly efficient high-harmonic generation in an orthogonally polarized two-color laser field *Physical Review Letters* 94, -.

Kling, M. F., Siedschlag, C., Verhoef, A. J., Khan, J. I., Schultze, M., Uphues, T., Ni, Y., Uiberacker, M., Drescher, M., Krausz, F. & Vrakking, M. J. J. (2006). Control of electron localization in molecular dissociation *Science* 312, 246-248.

Kubodera, S., Nagata, Y., Akiyama, Y., Midorikawa, K., Obara, M., Tashiro, H. & Toyoda, K. (1993). High-order harmonic-generation in laser-produced ions *Phys Rev A* 48, 4576-4582.

Liang, Y., Augst, S., Chin, S. L., Beaudoin, Y. & Chaker, M. (1994). High harmonic-generation in atomic and diatomic molecular gases using intense picosecond laser-pulses - a comparison *Journal of Physics B-Atomic Molecular and Optical Physics* 27, 5119-5130.

Lindner, F., Stremme, W., Schatzel, M., Grasbon, F., Paulus, G., Walther, H., Hartmann, R. & Struder, L. (2003). High-order harmonic generation at a repetition rate of 100 khz *Phys Rev A* 68, 013814.

Marques, M. A. L., Castro, A., Bertsch, G. F. & Rubio, A. (2003). Octopus: A first-principles tool for excited electron-ion dynamics *Computer Physics Communications* 151, 60-78.

Nabekawa, Y., Hasegawa, H., Takahashi, E. J. & Midorikawa, K. (2005). Production of doubly charged helium ions by two-photon absorption of an intense sub-10-fs soft x-ray pulse at 42 ev photon energy *Physical Review Letters* 94, -.

Niikura, H., Villeneuve, D. & Corkum, P. (2005). Mapping attosecond electron wave packet motion *Phys Rev Lett* 94, 083003.

Norreys, P., Zepf, M., Moustaizis, S., Fews, A., Zhang, J., Lee, P., Bakarezos, M., Danson, C., Dyson, A., Gibbon, P., Loukakos, P., Neely, D., Walsh, F., Wark, J. & Dangor, A. (1996). Efficient extreme uv harmonics generated from picosecond laser pulse interactions with solid targets *Phys. Rev. Lett.* 76, 1832-1835.

Perdew, J. P. & Zunger, A. (1981). Self-interaction correction to density-functional approximations for many-electron systems *Physical Review B (Condensed Matter)* 23, 5048.

Rundquist, A. (1998). Phase-matched generation of coherent soft x-rays *Science* 280, 1412-1415.

Runge, E. & Gross, E. K. U. (1984). Density-functional theory for time-dependent systems *Physical Review Letters* 52, 997.

Seres, J., Seres, E., Verhoef, A. J., Tempea, G., Strelill, C., Wobrauschek, P., Yakovlev, V., Scrinzi, A., Spielmann, C. & Krausz, F. (2005). Source of coherent kiloelectronvolt x-rays *Nature* 433, 596-596.

Suzuki, M., Baba, M., Ganeev, R., Kuroda, H. & Ozaki, T. (2006). Anomalous enhancement of a single high-order harmonic by using a laser-ablation tin plume at 47 nm *Optics Letters* 31, 3306-3308.

Taieb, R., Veniard, V., Wassaf, J. & Maquet, A. (2003a). Roles of resonances and recollisions in strong-field atomic phenomena. Ii. High-order harmonic generation *Phys Rev A* 68, 033403.

Taieb, R., Veniard, V., Wassaf, J. & Maquet, A. (2003b). Roles of resonances and recollisions in strong-field atomic phenomena. Ii. High-order harmonic generation *Physical Review A* 68, -.

Takahashi, E., Nabekawa, Y. & Midorikawa, K. (2002). Generation of 10-μj coherent extreme-ultraviolet light by use of high-order harmonics *Optics Letters*.

Tamaki, Y., Itatani, J., Nagata, Y., Obara, M. & Midorikawa, K. (1999). Highly efficient, phase-matched high-harmonic generation by a self-guided laser beam *Physical Review Letters* 82, 1422-1425.

Toma, E., Antoine, P., De Bohan, A. & Muller, H. (1999). Resonance-enhanced high-harmonic generation *J Phys B-At Mol Opt* 32, 5843-5852.

Troullier, N. & Martins, J. L. (1991). Efficient pseudopotentials for plane-wave calculations *Phys Rev B Condens Matter* 43, 1993-2006.

Wahlstrom, C., Borgstrom, S., Larsson, J. & Pettersson, S. (1995). High-order harmonic-generation in laser-produced ions using a near-infrared laser *Phys Rev A* 51, 585-591.
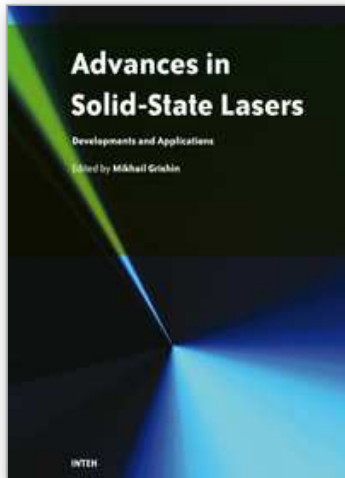
Advances in Solid State Lasers Development and Applications

Edited by Mikhail Grishin

Invention of the solid-state laser has initiated the beginning of the laser era. Performance of solid-state lasers improved amazingly during five decades. Nowadays, solid-state lasers remain one of the most rapidly developing branches of laser science and become an increasingly important tool for modern technology. This book represents a selection of chapters exhibiting various investigation directions in the field of solid-state lasers and the cutting edge of related applications. The materials are contributed by leading researchers and each chapter represents a comprehensive study reflecting advances in modern laser physics. Considered topics are intended to meet the needs of both specialists in laser system design and those who use laser techniques in fundamental science and applied research. This book is the result of efforts of experts from different countries. I would like to acknowledge the authors for their contribution to the book. I also wish to acknowledge Vedran Kordic for indispensable technical assistance in the book preparation and publishing.

How to reference

In order to correctly reference this scholarly work, feel free to copy and paste the following:

Tsuneyuki Ozaki, Rashid Ganeev, Masayuki Suzuki and Hiroto Kuroda (2010). High-Order Harmonic Generation from Low-Density Plasma, Advances in Solid State Lasers Development and Applications, Mikhail Grishin (Ed.), ISBN: 978-953-7619-80-0, InTech, Available from: http://www.intechopen.com/books/advances-in-solid-state-lasers-development-and-applications/high-order-harmonic-generation-from-low-density-plasma

INTECH
open science | open minds